ELSEVIER

Chemical Physics 276 (2002) 93–106

Chemical Physics

www.elsevier.com/locate/chemphys

# Ab initio study of the ammoniated ammonium ions $NH_4^+(NH_3)_{0-6}$

Bo-Cheng Wang[a,*], Jian-Chiang Chang[a], Jyh-Chiang Jiang[b], Sheng-Hsien Lin[b]

[a] *Department of Chemistry, Tamkang University, Tamsui 251, Taiwan*
[b] *Institute of Atomic and Molecular Sciences, Academia Sinica, P.O. Box 23-166, Taipei 107, Taiwan*

Received 15 June 2001

**Abstract**

The $NH_4^+(NH_3)_n$ $[n = 0–6]$ clusters have been studied using ab initio calculations. For $n = 0$ and 1, the geometry of clusters are optimized at B3LYP, MP2, CCD and QCISD levels with several basis sets, and the binding energies are compared to experimental results to find the reliable and less computationally demanding methods for the calculations of larger clusters. For $n = 2–6$, the geometry optimizations and NH stretching vibrational spectra are performed at B3LYP and MP2 levels with 6-31+G* basis set. The binding energies are corrected by basis set superposition errors (BSSE) and zero-point vibrational energies (ZPVE). These two approaches that correspondingly predict the filled first solvation shell are the lowest in energies at $n = 1–4$. The vibrational frequency shift of ammonium molecules have been investigated along with the frequency characteristics depending on the presence/absence of outer-shell ammonia molecules. In this study, the calculated binding energies and the characteristic NH stretching vibrational frequency shift are in good agreement with experimental data. In addition, the barriers of proton transfer between two heavy atoms and the internal rotation of ammonia molecular along the NH axis in $NH_4^+(NH_3)_n$ are estimated with several levels. 

## 1. Introduction

Studies of the structures and properties of cluster ion in the gas phase have been interesting for many decades. Molecular cluster ions can be handled more conveniently because their sizes are readily selected by mass spectrometric technique. Ion–solvent interactions play an important role in the ion chemistry of Earth's atmosphere which attract considerable attention [1–3]. Presently, a number of theoretical and experimental studies have focused their attention on investigating the changes in structural and spectral properties of small clusters in aqueous solutions with increasing cluster size [4–32]. However, the numbers of experimental spectra have been obtained, but many spectroscopic measurements are limited. As that so experiment spectra only have been confined in several small clusters [5–17]. Recently advance in ab initio calculations have allowed the structures, binding energies and vibrational frequencies of ion and molecular clusters to be predicted accurately [4], and the calculations are the useful reference for

* Corresponding author.

0301-0104/02/$ - see front matter 
PII: S0301-0104(01)00604-8

comparison with experiments [8–14]. Particularly, the density functional theory (DFT) has been generally used in studying extended systems, such as clusters.

The importance of tetrahedral ammonium ion in chemistry and biology is well established. In order to gain a better understanding of this cation, its gas-phase properties have attracted huge interest over the years. So far, many investigators contributed in this field to determine the enthalpy, $\Delta H^{\circ}$, for formation of the solvated ammonium ion $NH_4^+(NH_3)_n$ and $NH_4^+(H_2O)_n$. Previous thermochemical measurements revealed a smooth decrease in the heat of hydration $(-\Delta H_{n-1,n})$ for the clustering, $NH_4^+(H_2O)_{n-1} + H_2O \rightarrow NH_4^+(H_2O)_n$, as $n$ increases from 2 to 6; whereas, there exists an abrupt change between $-\Delta H_{3,4}$ and $-\Delta H_{4,5}$ in the $NH_3$ solvated case [18–20]. A number of structural isomers for $NH_4^+(H_2O)_{4-6}$ in a supersonic jet using vibrational predissociation spectroscopy (VPS) were identified [5,14]. The stable isomers of $NH_4^+(H_2O)_{1-5}$ were found by ab initio calculation [4]. Despite, exploration in how vibrational frequencies vary with cluster sizes has been made on $NH_4^+(NH_3)_n$ using VPS in a supersonic jet, most of the existing calculations concerns only the properties of $NH_4^+$ or computing with low level of theory [6,7,17]. The comparison between experiments and calculations is still deficient. In addition, the proton transfer in clusters remains one of the most important elementary reactions of chemistry. Within the field of gas-phase ion chemistry, a wide range of studies have dealt with solvation of protons in gas-phase clusters, yielding insight into the structures and energies of ionic microsolvent clusters [8–14].

In this study, we calculated the total interaction energies of the reaction, $NH_4^+ + nNH_3 \rightarrow NH_4^+(NH_3)_n$ and stepwise interaction energies of $NH_4^+(NH_3)_{n-1} + NH_3 \rightarrow NH_4^+(NH_3)_n$. Also explored in the calculations was the dependence of the structures, hydration energies and vibrational frequency shifts on the number of solvent molecules; how these properties are influenced by the presence of outer-shell solvent molecules was investigated. The barriers of proton transfer between two heavy atoms and the internal rotation of $NH_3$ molecule along the NH axis in the smaller ammoniated ammonium ions were estimated with several levels.

## 2. Calculation method

The ab initio calculations were performed in Gaussian 94 package [33]. For $NH_3$ molecule, $NH_4^+$ ion and $NH_4^+(NH_3)_{1-6}$ clusters, the equilibrium geometric parameters, vibrational frequencies and thermodynamic quantities were performed at the MP2 and B3LYP levels with 6-31+G* basis set. Whereas the basis set superposition error (BSSE) corrections to the binding energies were estimated using the counterpoise method of Boys and Bernaridi [34]. The binding energies for all optimized structures were both corrected by zero-point vibrational energy (ZPVE) and BSSE. The BSSE corrections for the stepwise and total binding energies were made as follows:

(1) The stepwise binding energies, $NH_4^+(NH_3)_{n-1} + NH_3 \rightarrow NH_4^+(NH_3)_n$

$$E(\mathrm{BSSE}) = \{E[NH_4^+(NH_3)_{n-1}]_n - E[NH_4^+(NH_3)_{n-1}]\} + \{E[NH_4^+(NH_3)_n] - E[NH_3]\}.$$

(2) The stepwise binding energies, $NH_4^+ + nNH_3 \rightarrow NH_4^+(NH_3)_n$

$$E(\mathrm{BSSE}) = \{E[NH_4^+]_n - E[NH_4^+]\} + \sum_{i=1}^{n} \{E[(NH_3)_i]_n - E[(NH_3)_i]\},$$

where $E[NH_4^+(NH_3)_{n-1}]_n$, $E[(NH_3)_i]_n$ and $E[NH_4^+]_n$ represent the calculated energies of $NH_4^+(NH_3)_{n-1}$, $(NH_3)_i$ and $NH_4^+$ considering their geometries within the clusters, and $E[NH_4^+(NH_3)_{n-1}]$, $E[NH_3]_i$ and $E[NH_4^+]$ are the energies of the individual clusters and ions with the basis functions centered on themselves.

A complete set of basis functions was employed to describe $NH_4^+(NH_3)_n$. The calculation of the potential energies of proton transfer between two heavy atoms are estimated at the B3LYP, MP2, CCD and QCISD levels with 6-31+G* and 6-311++G** basis sets. The potential surface of proton transfer is scanned against the difference of

NH bond length at interval of 0.02 Å from barriers to equilibrium geometry. The internal rotation of ammonia along the $C_3$ axis $NH_4^+NH_3$ is estimated at the B3LYP, MP2, CCD and QCISD levels with 6-31+G* basis set. The potential energy of internal rotation is estimated by the change of the torsional angle at an interval of 10° from 0° to 120°.

## 3. Results and discussion

### 3.1. Energetics and geometries

According to the analysis of the geometric structures, there are various structural arrangements of $NH_4^+(NH_3)_n$ $[n = 1–6]$ clusters presented in Fig. 1 with symmetry consideration. Each structure is shown by the notation $(n_1 + n_2 + n_3)$, in which $n_1, n_2$ and $n_3$ denote the number of $NH_3$ subunit in the first, second and third solvation shell, respectively. The experimental results lead to the conclusion that the formation of ammoniated ammonium ions $NH_4^+(NH_3)_n$ is $NH_4^+(NH_3)_{n-1} + NH_3 \rightarrow NH_4^+(NH_3)_n$ reaction series. Table 1 shows the calculated geometrical parameters for $NH_4^+(NH_3)_{0–6}$ clusters at B3LYP/6-31+G* and MP2/6-31+G* levels. In order to compare the calculated results, both the B3LYP/6-31+G* and MP2/6-31+G* values are listed, where the latter are given in the parentheses. The calculated bond length of NH in $NH_4^+$ ion and in $NH_3$ molecule are 1.027 (1.027) and 1.016 (1.016) Å, respectively. Two important parameters, the NH bond length, and the distance of $NH\cdots N$ in the $NH_4^+(NH_3)_n$ clusters are closely related to the interactions in the $NH_4^+(NH_3)_n$ clusters. The total energies ($E$) and the corrected energies ($E_{ZPVE}$ and $E_f$) obtained from ab initio calculations with B3LYP/6-31+G* and MP2/6-31+G* for $NH_4^+(NH_3)_n$ clusters are presented in Table 2. Also, the total interaction energies and the stepwise interaction energies are given in Table 4.

#### 3.1.1. $NH_4^+(NH_3)$ cluster

1I is the smallest ionic cluster in the $NH_4^+(NH_3)_n$ clusters which is solvated by a single ammonia. Fig. 1 shows two possible isomeric structures, 1I and 1II, of $NH_4^+(NH_3)$ cluster which belong to the $C_{3v}$ and $D_{3d}$ symmetry, respectively. In 1991, Lee and coworkers [7] proposed that the most possible structure for $NH_4^+(NH_3)$ cluster is $D_{3d}$ symmetry. In this work, ab initio calculations with B3LYP/6-31+G* and MP2/6-31+G* levels predict that 1I ($C_{3v}$) is the minimum energy isomer in $NH_4^+(NH_3)$ cluster. For 1I cluster, two $NH_3$ subunits are located in eclipsed conformation. Table 3 compares the binding energies with and without the BSSE and ZPVE corrections of isomer 1I at various computational levels. They are performed in an effort to find a reliable and economical method for predicting the properties of larger clusters. The calculated final interaction energy at the higher levels is found to converge at $-E_f \sim 22.5$ kcal/mol, a value which is slightly overestimated by MP2 using the 6-31+G*, 6-31++G**, 6-311+G** and 6-311++G** basis sets. It appears that use of basis sets that are more flexible than 6-31+G* does not substantially improve the accuracy of the MP2 calculations. However, if diffuse functions are not imposed on the heavy atoms, considerable overestimation of the hydration energy can be made by MP2. As for DFT, using the same basis sets, the B3LYP overestimates the interaction energy more than 2 kcal/mol. Similar to that of MP2, the use of more flexible basis sets only slightly improves the results of this calculation. A comparison of the calculated with the measured values shown in Table 3 reveals that the MP2/6-31+G* method can provide sufficiently accurate estimates for the interaction energy of $NH_4^+$ and $NH_3$. However, the application of this method to larger clusters is somewhat impractical at present since extensive disk space is required. Jiang et al. [4] concluded from systematic comparisons of the calculations in predicting the interaction energies of $NH_4^+$ and $H_2O$ in the $NH_4^+(H_2O)_n$ clusters that the B3LYP/6-31+G* can be an alternative since the DFT-predicted interaction energies agree well with those of MP2/6-31+G* at a larger $n$. Therefore, to test the validity of the B3LYP method in elucidating ion–molecule interactions, calculations at both the B3LYP/6-31+G* and MP2/6-31+G* levels were performed and compared for clusters with a size of $n = 2–6$.

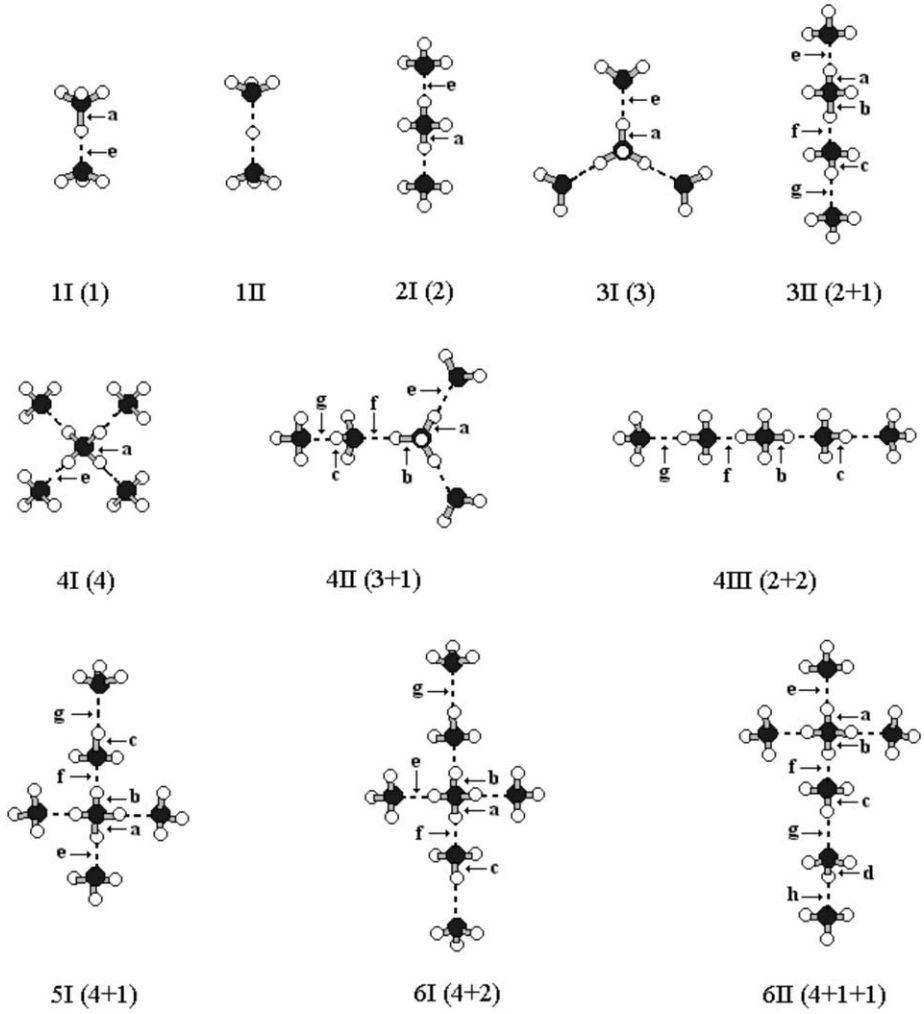


Fig. 1. Ab initio optimized structures of $NH_4^+(NH_3)_{1-6}$. The N and H atoms are denoted by • and ○, respectively.

According to ab initio calculation, 1II ($D_{3d}$ isomer) should be a transition structure of proton transfer and it is higher in energy by 0.5 kcal/mol (B3LYP/6-31+G* level) than 1I ($C_{3v}$) isomer. In the $D_{3d}$ structure, two $NH_3$ subunits equally share the $H^+$ proton and which are in the staggered conformation. Fig. 2 shows the potential surface of proton transfer between two heavy atoms in the $NH_4^+(NH_3)$. The prediction of the barrier, which is found to converge at 2.7 kcal/mol by the higher level calculation (QCISD/6-311++G**), is significantly underestimated at the B3LYP/6-31+G* level, whereas, it is about 1 kcal/mol underestimated at the MP2/6-31+G* level.

From the geometrical optimization of structure 1I isomer, the calculated bond length of bonded NH (b-NH) and free NH (f-NH) in the $NH_4^+$ ion are found 1.138 (1.098) and 1.025 (1.025) Å at B3LYP (MP2) level, respectively, in Table 1. Particularly, this elongation of b-NH is due to hydrogen bonding interacting in $NH_4^+(NH_3)$ cluster. The distance of $NH\cdots N$ is 1.571 (1.675) Å, which is considerably shorter than the typical separation of $\sim 3$ Å in neutral van der Waals complexes.

Nearly free internal rotation of $NH_3$ molecules about their local $C_3$ axes in the first solvation shell was observed in the $NH_4^+(NH_3)_{1-6}$ clusters by VPS [7]. We also predicted the internal rotational

Table 1
Calculated geometrical parameters for $NH_4^+(NH_3)_{0-6}$ clusters[A,B]

| Symmetry<br>Structure | $C_{3v}$<br>1I | $C_{2v}$<br>2I | $C_{3v}$<br>3I | $C_s$<br>3II | $T_d$<br>4I | $C_s$<br>4II | $C_{2v}$<br>4III | $C_s$<br>5I | $C_{2v}$<br>6I | $C_s$<br>6II |
|---|---|---|---|---|---|---|---|---|---|---|
| *$NH_4^+$ ion* | | | | | | | | | | |
| b-NH[a] | 1.138 | 1.078 | 1.059 | 1.068 | 1.049 | 1.055 | | 1.047 | 1.044 | 1.045 |
| | (1.098) | (1.065) | (1.051) | (1.059) | (1.047) | (1.048) | | (1.042) | (1.040) | (1.041) |
| $b^{\#}$-NH[b] | | | | 1.111 | | 1.076 | 1.092 | 1.060 | 1.056 | 1.064 |
| | | | | (1.086) | | (1.063) | (1.076) | (1.051) | (1.049) | (1.054) |
| $f^*$-NH | 1.025 | 1.024 | 1.023 | 1.023 | | 1.023 | 1.023 | | | |
| | (1.025) | (1.024) | (1.023) | (1.023) | | (1.022) | (1.023) | | | |
| *First-shell $NH_3$* | | | | | | | | | | |
| f-NH | 1.023 | 1.022 | 1.021 | 1.021 | 1.021 | 1.021 | | 1.020 | 1.020 | 1.020 |
| | (1.022) | (1.022) | (1.021) | (1.021) | (1.021) | (1.021) | | (1.020) | (1.020) | (1.020) |
| $b^*$-NH[c] | | | | 1.039 | | 1.035 | 1.037 | 1.033 | 1.032 | 1.037 |
| | | | | (1.034) | | (1.031) | (1.033) | (1.030) | (1.029) | (1.033) |
| $f^*$-NH | | | | 1.022 | | 1.021 | 1.021 | 1.021 | 1.021 | 1.021 |
| | | | | (1.021) | | (1.021) | (1.021) | (1.021) | (1.021) | (1.021) |
| *Second-shell $NH_3$* | | | | | | | | | | |
| f-NH | | | | | | 1.020 | 1.020 | 1.020 | 1.020 | |
| | | | | | | (1.020) | (1.020) | (1.020) | (1.020) | |
| $b^*$-NH[d] | | | | | | | | | | 1.030 |
| | | | | | | | | | | (1.028) |
| $f^*$-NH | | | | | | | | | | 1.020 |
| | | | | | | | | | | (1.020) |
| *Third-shell $NH_3$* | | | | | | | | | | |
| f-NH | | | | | | | | | | 1.020 |
| | | | | | | | | | | (1.020) |
| *$NH_4^+$ ion* | | | | | | | | | | |
| $NH\cdots N$[e] | 1.571 | 1.754 | 1.848 | 1.801 | 1.920 | 1.875 | | 1.938 | 1.954 | 1.945 |
| | (1.675) | (1.806) | (1.886) | (1.840) | (1.947) | (1.907) | | (1.962) | (1.975) | (1.960) |
| $NH^{\#}\cdots N$[f] | | | | 1.632 | | 1.756 | 1.691 | 1.844 | 1.865 | 1.815 |
| | | | | (1.706) | | (1.804) | (1.745) | (1.879) | (1.895) | (1.855) |
| *First-shell $NH_3$* | | | | | | | | | | |
| $NH\cdots N$[g] | | | | 2.014 | | 2.060 | 2.038 | 2.098 | 2.106 | 2.028 |
| | | | | (2.069) | | (2.102) | (2.084) | (2.130) | (2.139) | (2.069) |
| *Second-shell $NH_3$* | | | | | | | | | | |
| $NH\cdots N$[h] | | | | | | | | | | 2.127 |
| | | | | | | | | | | (2.159) |

b-NH: bonded NH; $b^{\#}$-NH: bonded NH with neighboring $NH_3$ subunit; f-NH: nonbonded NH; $f^*$-NH: nonbonded NH with neighboring shell $NH_3$ subunit; $NH\cdots N$: the distance between H and N with neighboring $NH_3$ subunit; $NH^{\#}\cdots N$: the distance between H and N without neighboring $NH_3$ subunit.

[A] The bond lengths are in unit of Å.

[B] Bonds a–h are denoted in Fig. 1.

Table 2
Energies ($E_h$) of $NH_4^+(NH_3)_n$ at $n = 0$–6

| Spices | B3LYP/6-31+G* | | | MP2/6-31+G* | | |
|---|---|---|---|---|---|---|
| | $E$ | $E_{ZPVE}$[a] | $E_f$[b] | $E$ | $E_{ZPVE}$[a] | $E_f$[b] |
| $NH_3$ | −56.55699 | −56.52247 | | −56.36320 | −56.32806 | |
| $NH_4^+$ | −56.89459 | −56.84469 | | −56.70117 | −56.65068 | |
| 1I | −113.49808 | −113.41118 | −113.40858 | −113.10849 | −113.01976 | −113.01512 |
| 2I | −170.08882 | −169.96341 | −169.95850 | −169.50609 | −169.37853 | −169.37008 |
| 3I | −226.67300 | −226.50973 | −226.50267 | −225.89791 | −225.73200 | −225.71945 |
| 3II | −226.66411 | −226.50182 | −226.49494 | −225.88769 | −225.72244 | −225.71018 |
| 4I | −283.25231 | −283.05112 | −283.04193 | −282.28538 | −282.08165 | −282.06534 |
| 4II | −283.24586 | −283.04527 | −283.03640 | −282.27747 | −282.07379 | −282.05790 |
| 4III | −283.23802 | −283.03823 | −283.02953 | −282.26823 | −282.06516 | −282.04947 |
| 5I | −339.82307 | −339.58544 | −339.57470 | −338.66312 | −338.42173 | −338.40223 |
| 6I | −396.39325 | −396.11876 | −396.10634 | −395.04030 | −394.76129 | −394.73857 |
| 6II | −396.39164 | −396.11691 | −396.10436 | −395.03859 | −394.75946 | −394.73667 |

[a] With ZPVE corrections.
[b] With both ZPVE and BSSE corrections.

Table 3
The calculated first hydration energy (kcal/mol) of $NH_4^+NH_3$

| Method | $-\Delta E$ | $-\Delta E_{ZPVE}$[a] | $-\Delta E_{cp}$[b] | $-\Delta E_f$[c] |
|---|---|---|---|---|
| B3LYP/6-31G* | 33.50 | 32.22 | 32.21 | 30.93 |
| B3LYP/6-31G** | 33.74 | 32.72 | 32.36 | 31.35 |
| B3LYP/6-31+G* | 29.18 | 27.61 | 27.55 | 25.99 |
| B3LYP/6-31++G** | 29.15 | 27.81 | 27.81 | 26.48 |
| B3LYP/6-311++G* | 29.13 | 27.42 | 27.23 | 25.52 |
| B3LYP/6-311+G** | 28.29 | 26.93 | 27.27 | 25.91 |
| B3LYP/6-311++G** | 28.67 | 26.88 | 27.66 | 25.87 |
| MP2/6-31G* | 31.16 | 29.32 | 28.92 | 27.08 |
| MP2/6-31+G* | 27.69 | 25.73 | 24.78 | 22.83 |
| MP2/6-31G** | 31.34 | 29.90 | 29.00 | 27.56 |
| MP2/6-31++G** | 27.52 | 25.92 | 24.86 | 23.26 |
| MP2/6-311+G** | 27.56 | 25.97 | 25.11 | 23.52 |
| MP2/6-311++G** | 27.55 | 26.00 | 25.07 | 23.52 |
| MP4(DQ)/6-311++G**[a] | 26.32 | 24.91 | 24.07 | 22.65 |
| MP4(SDQ)/6-311++G**[a] | 26.44 | 24.90 | 24.15 | 22.62 |
| CCD/6-311++G**[a] | 26.24 | 24.75 | 24.01 | 22.52 |
| QCISD/6-311++G**[a] | 26.35 | 24.71 | 24.09 | 22.44 |
| Expt. | | 25.4 [36], 24.8 [19], 21.5 [37], 27.0 [38] | | |

[a] With ZPVE corrections.
[b] With BSSE corrections.
[c] With both ZPVE and BSSE corrections.

motion with several levels. Fig. 3 displays the calculated potential surface of internal rotation of $NH_3$ molecules about their local $C_3$ axes in the $NH_4^+(NH_3)$ by several levels. The calculated barrier is about 12 $cm^{-1}$ which is in agreement with experimental prediction 10 $cm^{-1}$ [7].

*3.1.2. $NH_4^+(NH_3)_2$ clusters*

For the isomer 2I of $NH_4^+(NH_3)_2$ cluster, two $NH_3$ subunits interact with $NH_4^+$ ion by hydrogen bonding in the first solvation shell. The symmetry analysis reveals that 2I is the only possible structure for $n = 2$ cluster, whereas, our calculation

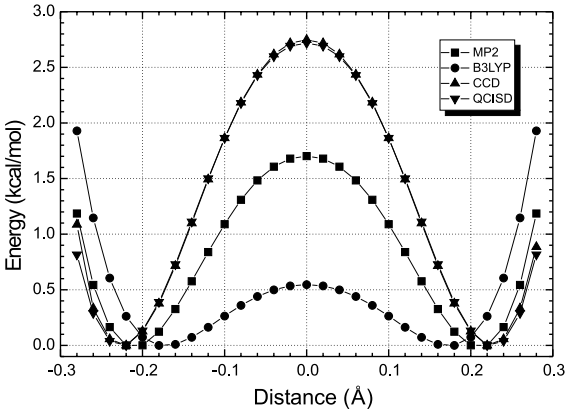


Fig. 2. Calculated potential surface of proton transfer between two heave atom in $NH_4^+NH_3$.

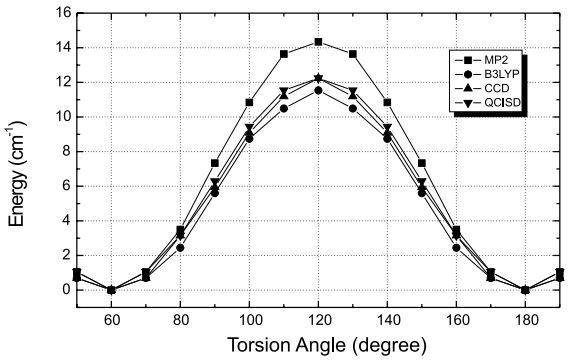


Fig. 3. Calculated potential surface of internal rotation of $NH_3$ molecular about local $C_3$ axes in $NH_4^+NH_3$.

shows an optimized $NH_4^+(NH_3)_2$ structure with bent $C_{2v}$ symmetry, which has been obtained by Hirao et al. [17] with ab initio calculation also. The predicted bond lengths of the b-NH ($NH_4^+$ ion) and of the distance of NH···N are 1.078 (1.065) and 1.754 (1.806) Å, respectively (Table 1). In 2I, the bond length of each b-NH is slightly decreased by $\sim 0.060$ (0.033) Å, and the NH···N distances are increased by $\sim 0.183$ (0.131) Å, compared to those of $NH_4^+(NH_3)$. The interaction energy of the addition of $NH_3$ to $NH_4^+(NH_3)$ is 17.15 (16.49) kcal/mol, which is much less than the interaction energy 25.99 (22.83) kcal/mol of $[NH_3 + NH_4^+ \rightarrow NH_4^+(NH_3)]$ in Table 4. The two NH···N interactions are anti-cooperative (the interaction energy is negatively nonadditive when the second $NH_3$ molecule attaches to the ion), which cause the b-NH bonds, shorten, the NH···N distances increase.

### 3.1.3. $NH_4^+(NH_3)_3$ cluster

Fig. 1 shows two possible $NH_4^+(NH_3)_3$ clusters 3I and 3II, which have $C_{3v}$ and $C_s$ symmetries, respectively. In isomer 3I, the three first shell $NH_3$ subunits associate with the hydrogen bond on the central ammonium ion. The other $NH_4^+(NH_3)_3$ ($C_s$) (2 + 1) cluster contains two first shell $NH_3$ subunits and one second shell $NH_3$ subunit as almost linear conformation. The B3LYP/6-31+G* calculation predicts that isomer 3I with $C_{3v}$ symmetry is 4.85 kcal/mol lower in energy than the

Table 4
Total and stepwise hydration energies (kcal/mol) of $[NH_4^+ + nNH_3 \rightarrow NH_4^+(NH_3)_n]$ and $[NH_4^+(NH_3)_{n-1} + nNH_3 \rightarrow NH_4^+(NH_3)_n]$ estimated by B3LYP/6-31+G* and MP2/6-31+G*

| Spices | B3LYP/6-31+G* | | MP2/6-31+G* | |
|---|---|---|---|---|
| | $-\Delta E_n$[a] | $-\Delta E_{n-1,n}$[a,b] | $-\Delta E_n$[a] | $-\Delta E_{n-1,n}$[a,b] |
| 1I | 25.99 | | 22.83 | |
| 2I | 43.21 | 17.15 (1I) | 39.71 | 16.49 (1I) |
| 3I | 56.83 | 13.51 (2I) | 53.08 | 13.18 (2I) |
| 3II | 51.98 | 8.83 (2I) | 47.26 | 7.85 (2I) |
| 4I | 67.37 | 10.33 (3I) | 64.27 | 10.74 (3I) |
| 4II | 63.90 | 7.12 (3I) | 59.60 | 6.61 (3I) |
| 4III | 59.59 | 7.63 (3II) | 54.31 | 7.14 (3II) |
| 5I | 73.83 | 6.40 (4I) | 69.80 | 5.61 (4I) |
| 6I | 79.59 | 5.78 (5I) | 75.00 | 5.30 (5I) |
| 6II | 78.34 | 4.66 (5I) | 73.81 | 4.20 (5I) |

[a] With both BSSE and ZPVE corrections.
[b] Notations in parentheses denoting the isomers of $NH_4^+(NH_3)_{n-1}$.

isomer 3II with $C_s$ symmetry (Table 4). Although isomer 3II has the same hydrogen bonds as 3I, it is one H-bond less in the first shell which is ionic hydrogen bonding, and is relatively not favored in energy. Conclusively, $NH_4^+(NH_3)_3$ ($C_{3v}$) is the lowest energy structure in $NH_4^+(NH_3)_3$ cluster, which is in accord with experimental prediction by Lee and coworkers [4]. According to the ab initio calculations, the bond lengths of b-NH in $NH_4^+$ and the distance of $NH\cdots N$ in $NH_4^+(NH_3)_3$ ($C_{3v}$) are 1.059 (1.051) and 1.848 (1.886) Å, respectively. Compared to 2I and 1I, this isomer has a shorter b-NH bond length, accompanied by an increased $NH\cdots N$ distance.

Does $N_2H_7^+$ exist in the ammoniated ammonium ions is one of the interests in this study. Ab initio calculations of $H^+(H_2O)_n$ indicated that the $H_5O_2^+(H_2O)_{n-2}$ isomers, which are highly symmetric, become favorable in energy as cluster size increases [13]. Especially, $H_5O_2^+(H_2O)_4$ was found to be the most stable species in the $H^+(H_2O)_6$ isomers [13]. Particularly, in the exploration of cyclic $H^+(CH_3OH)_5$, the spectroscopic evidence of symmetric proton stabilization in between two solvated methanol molecules was observed [8]. We also considered $N_2H_7^+(NH_3)_2$ species, but our calculation indicates that it is the transition state of the proton transfer in 3II. The barrier is 1.88 kcal/mol estimated at QCISD/6-311++G**//B3LYP/6-311++G** level. Compared to $NH_4^+(NH_3)$, this barrier is only a little decreased.

### 3.1.4. $NH_4^+(NH_3)_4$ cluster

In the case of $n = 4$ cluster, 4I ($T_d$) (4), 4II ($C_s$) (3 + 1) and 4III ($C_{2v}$) (2 + 2) have been considered for the possible structures of $NH_4^+(NH_3)_4$ clusters (Fig. 1). 4I represents the completion of the first solvation shell on the $NH_4^+$ ion. 4II contains three first shell $NH_3$ subunits that interact with $NH_4^+$ ion and one second shell $NH_3$ subunit. This cluster form hydrogen bonding to its own primary subunit. 4III shows that the $NH_4^+$ ion is in a linear interaction with two first shell $NH_3$ subunits and two second shell $NH_3$ subunits.

The B3LYP/6-31+G* calculation shows that 4I is more stable than 4II and 4III by 3.47 and 7.78 kcal/mol, respectively (Table 4). It demonstrates that the isomer with more number of the first shell H-bonds is more stable. Since the most stable isomer of $NH_4^+(NH_3)_4$ cluster belongs to the $T_d$ symmetry, its four NH in $NH_4^+$ should almost be equal. Theoretically, the bond length of NH in $NH_4^+$ decreased to 1.049 (1.047) Å and the distance of hydrogen bonding increased to 1.920 (1.947) Å. The bond lengths of NH in $NH_4^+$ and the $NH\cdots N$ distances are continuously decreased and increased, respectively, from 1I to 4I. The respective stepwise hydration energies of ($NH_4^+ + NH_3 \rightarrow 1I$), ($1I + NH_3 \rightarrow 2I$), ($2I + NH_3 \rightarrow 3I$) and ($3I + NH_3 \rightarrow 4I$) are all also monotonously decreased. These properties reflect that both the charge delocalization of the ion and the hydrogen-bond anti-cooperativity are reinforced by the extra $NH\cdots N$ formation.

### 3.1.5. $NH_4^+(NH_3)_5$ cluster

The most stable species is the first solvation shell filled completely at $n = 4$ with a tetrahedral symmetry. One additional $NH_3$ solvent molecule binds to successive first shell ammoniate. Only 5I with $C_s$ symmetry is proposed in this paper as the addition of the fifth $NH_3$ solvent molecule to 4I. Two data sets concerning the bond length of b-NH and the distance of $NH\cdots N$ exist for 5I in the first solvation shells. In one set where the interaction of $NH\cdots N$ hydrogen bond is cooperative with that of the second shell $NH\cdots N$, the b-NH bond, 1.060 (1.051) Å, is lengthened, and the $NH\cdots N$ distance, 1.844 (1.879) Å, is shortened, compared to those in 4I. In another set without the second solvation shell, the bond length of b-NH bond and the distance of $NH\cdots N$ is slightly decreased and increased, respectively, compared to those in 4I. It demonstrates that the second shell solvation causes the unsymmetrical charge delocalization of ion. As far to the second shell solvation, it involves bonding of the ammonium dimer to the ion, where one of the first shell $NH_3$ is both as proton donor and as proton acceptor in a linear linkage, the strength of each $NH\cdots N$ ($NH_4^+$ ion) and $NH\cdots N$ ($NH_3\cdots NH_3$) hydrogen bond is augmented due to the concerted coupling. Compared to ammonium dimer, the bond length of b-NH bond and the distance of $NH\cdots N$ of the $NH_3\cdots NH_3$ in 5I is significantly increased and decreased by 0.03 (0.01) and 0.29 (0.10) Å, respectively [35].

Table 5
Frequencies ($cm^{-1}$) and absorption intensities (km/mol) of NH stretches of $NH_3, NH_4^+$ and $NH_4^+(NH_3)_n$ at $n = 1$–6

| Spices | B3LYP/6-31+G* | | MP2/6-31+G* | | Vibration mode |
|---|---|---|---|---|---|
| | Scaled freq. | Int. | Scaled freq. | Int. | |
| $NH_3$ | 3459.1 | 2.0 | 3507.1 | 0.8 | |
| | 3596.0 | 2.5 | 3669.5 | 7.4 | |
| | 3596.0 | 2.5 | 3669.5 | 7.4 | |
| $NH_4^+$ | 3367.8 | 0.0 | 3390.8 | 0.0 | |
| | 3483.8 | 194.6 | 3535.3 | 211.9 | |
| | 3483.8 | 194.6 | 3535.3 | 211.9 | |
| | 3483.8 | 194.6 | 3535.3 | 211.9 | |
| 1I | 1797.3 | 3148.0 | 2305.4 | 2568.5 | $\nu_b(NH)_i$ |
| | 3427.6 | 54.9 | 3455.7 | 82.5 | $\nu_f(NH)_i$ |
| | 3444.0 | 5.8 | 3475.5 | 3.9 | $\nu_f(NH)_I$ |
| | 3532.8 | 107.2 | 3577.3 | 135.1 | $\nu_f(NH)_i$ |
| | 3532.8 | 107.2 | 3577.3 | 135.1 | $\nu_f(NH)_n$ |
| | 3553.6 | 42.8 | 3606.3 | 44.8 | $\nu_f(NH)_n$ |
| | 3553.6 | 42.8 | 3606.3 | 44.8 | $\nu_f(NH)_n$ |
| 2I | 2559.4 | 2956.7 | 2814.1 | 2446.4 | $\nu_b(NH)_i$ |
| | 2637.0 | 967.4 | 2832.4 | 810.8 | $\nu_b(NH)_i$ |
| | 3448.7 | 5.9 | 3480.4 | 5.6 | $\nu_f(NH)_i$ |
| | 3448.8 | 4.0 | 3480.4 | 4.4 | $\nu_f(NH)_i$ |
| | 3475.0 | 71.6 | 3515.8 | 105.8 | $\nu_f(NH)_n$ |
| | 3545.2 | 75.7 | 3594.8 | 97.7 | $\nu_f(NH)_n$ |
| | 3561.0 | 16.0 | 3614.5 | 19.8 | $\nu_f(NH)_n$ |
| | 3561.1 | 37.9 | 3614.5 | 46.6 | $\nu_f(NH)_n$ |
| | 3562.5 | 0.0 | 3616.4 | 0.0 | $\nu_f(NH)_n$ |
| | 3562.7 | 51.6 | 3616.6 | 63.9 | $\nu_f(NH)_n$ |
| 3I | 2878.7 | 1969.6 | 3030.1 | 222.1 | $\nu_b(NH)_i$ |
| | 2878.7 | 969.6 | 3062.8 | 652.6 | $\nu_b(NH)_i$ |
| | 2901.7 | 265.5 | 3062.8 | 1652.6 | $\nu_b(NH)_i$ |
| | 3450.4 | 2.0 | 3482.3 | 1.9 | $\nu_f(NH)_i$ |
| | 3450.4 | 2.0 | 3482.3 | 1.9 | $\nu_f(NH)_n$ |
| | 3450.6 | 0.5 | 3482.4 | 0.7 | $\nu_f(NH)_n$ |
| | 3520.1 | 61.7 | 3569.7 | 87.5 | $\nu_f(NH)_n$ |
| | 3565.6 | 0.0 | 3619.9 | 0.0 | $\nu_f(NH)_n$ |
| | 3565.8 | 19.3 | 3620.0 | 30.7 | $\nu_f(NH)_n$ |
| | 3565.8 | 19.3 | 3620.0 | 30.7 | $\nu_f(NH)_n$ |
| | 3565.9 | 12.9 | 3620.2 | 12.1 | $\nu_f(NH)_n$ |
| | 3565.9 | 12.9 | 3620.2 | 12.1 | $\nu_f(NH)_n$ |
| | 3566.0 | 52.7 | 3620.3 | 70.6 | $\nu_f(NH)_n$ |
| 4I | 3039.0 | 0.0 | 3134.3 | 0.0 | $\nu_b(NH)_i$ |
| | 3062.6 | 392.1 | 3209.0 | 186.6 | $\nu_b(NH)_i$ |
| | 3062.6 | 1392.1 | 3209.0 | 1186.6 | $\nu_b(NH)_i$ |
| | 3062.6 | 1392.1 | 3209.0 | 1186.6 | $\nu_b(NH)_i$ |
| | 3452.0 | 0.5 | 3484.5 | 0.4 | $\nu_f(NH)_n$ |
| | 3452.0 | 0.5 | 3484.5 | 0.4 | $\nu_f(NH)_n$ |
| | 3452.0 | 0.5 | 3484.5 | 0.4 | $\nu_f(NH)_n$ |
| | 3452.2 | 0.0 | 3484.5 | 0.0 | $\nu_f(NH)_n$ |
| | 3569.9 | 0.0 | 3624.8 | 0.0 | $\nu_f(NH)_n$ |
| | 3569.9 | 0.0 | 3624.8 | 0.0 | $\nu_f(NH)_n$ |
| | 3569.9 | 0.0 | 3624.9 | 0.0 | $\nu_f(NH)_n$ |
| | 3569.9 | 0.0 | 3624.9 | 0.0 | $\nu_f(NH)_n$ |

Table 5 (*continued*)

| Spices | B3LYP/6-31+G* | | MP2/6-31+G* | | Vibration mode |
|---|---|---|---|---|---|
| | Scaled freq. | Int. | Scaled freq. | Int. | |
| | 3569.9 | 0.0 | 3624.9 | 0.0 | $\nu_f(NH)_n$ |
| | 3570.1 | 40.5 | 3625.0 | 57.5 | $\nu_f(NH)_n$ |
| | 3570.1 | 40.5 | 3625.0 | 57.5 | $\nu_f(NH)_n$ |
| | 3570.1 | 40.5 | 3625.0 | 57.5 | $\nu_f(NH)_n$ |
| 5I | 2873.0 | 1517.1 | 3041.8 | 1007.9 | $\nu_b(NH)_i$ |
| | 3077.4 | 366.9 | 3183.8 | 550.1 | $\nu_b(NH)_i$ |
| | 3104.0 | 1235.5 | 3242.3 | 1080.6 | $\nu_b(NH)_i$ |
| | 3106.9 | 1263.8 | 3244.6 | 1087.6 | $\nu_b(NH)_i$ |
| | 3304.0 | 356.9 | 3389.8 | 239.7 | $\nu_b(NH)_n$ |
| | 3452.4 | 0.2 | 3485.3 | 0.1 | $\nu_f(NH)_n$ |
| | 3452.8 | 0.2 | 3485.7 | 0.1 | $\nu_f(NH)_n$ |
| | 3452.9 | 0.1 | 3485.7 | 0.1 | $\nu_f(NH)_n$ |
| | 3452.9 | 0.1 | 3488.4 | 0.1 | $\nu_f(NH)_n$ |
| | 3498.4 | 49.1 | 3556.0 | 86.3 | $\nu_f(NH)_n$ |
| | 3559.9 | 6.6 | 3618.8 | 11.5 | $\nu_f(NH)_n$ |
| | 3570.8 | 12.3 | 3626.6 | 17.9 | $\nu_f(NH)_n$ |
| | 3570.8 | 10.8 | 3626.7 | 13.1 | $\nu_f(NH)_n$ |
| | 3571.5 | 10.5 | 3627.2 | 13.1 | $\nu_f(NH)_n$ |
| | 3571.6 | 21.4 | 3627.2 | 36.8 | $\nu_f(NH)_n$ |
| | 3571.8 | 0.6 | 3627.8 | 3.0 | $\nu_f(NH)_n$ |
| | 3571.9 | 28.4 | 3627.9 | 38.6 | $\nu_f(NH)_n$ |
| | 3573.6 | 10.0 | 3633.5 | 15.5 | $\nu_f(NH)_n$ |
| | 3576.2 | 8.7 | 3635.7 | 13.9 | $\nu_f(NH)_n$ |
| 6I | 2923.6 | 2044.7 | 3068.7 | 427.9 | $\nu_b(NH)_i$ |
| | 2935.2 | 743.2 | 3096.4 | 716.2 | $\nu_b(NH)_i$ |
| | 3120.5 | 607.8 | 3235.6 | 717.1 | $\nu_b(NH)_i$ |
| | 3145.8 | 1156.5 | 3275.8 | 1002.9 | $\nu_b(NH)_i$ |
| | 3311.8 | 524.2 | 3395.4 | 324.7 | $\nu_b(NH)_n$ |
| | 3314.0 | 162.1 | 3396.8 | 132.4 | $\nu_b(NH)_n$ |
| | 3453.4 | 0.1 | 3486.7 | 0.0 | $\nu_f(NH)_n$ |
| | 3453.4 | 0.1 | 3486.8 | 0.0 | $\nu_f(NH)_n$ |
| | 3453.6 | 0.1 | 3488.8 | 0.0 | $\nu_f(NH)_n$ |
| | 3453.7 | 0.0 | 3488.8 | 0.1 | $\nu_f(NH)_n$ |
| | 3499.8 | 74.5 | 3559.1 | 119.0 | $\nu_f(NH)_n$ |
| | 3500.1 | 27.5 | 3559.3 | 57.0 | $\nu_f(NH)_n$ |
| | 3560.6 | 0.0 | 3620.7 | 0.0 | $\nu_f(NH)_n$ |
| | 3560.7 | 11.9 | 3620.8 | 21.9 | $\nu_f(NH)_n$ |
| | 3573.1 | 8.5 | 3629.4 | 12.7 | $\nu_f(NH)_n$ |
| | 3573.1 | 17.2 | 3629.5 | 25.8 | $\nu_f(NH)_n$ |
| | 3574.0 | 0.0 | 3630.0 | 0.0 | $\nu_f(NH)_n$ |
| | 3574.1 | 25.9 | 3630.2 | 38.4 | $\nu_f(NH)_n$ |
| | 3575.2 | 2.4 | 3634.6 | 4.1 | $\nu_f(NH)_n$ |
| | 3575.2 | 16.8 | 3634.6 | 26.2 | $\nu_f(NH)_n$ |
| | 3576.9 | 0.0 | 3636.5 | 0.0 | $\nu_f(NH)_n$ |
| | 3576.9 | 16.6 | 3636.5 | 26.9 | $\nu_f(NH)_n$ |

### *3.1.6. $NH_4^+$ $(NH_3)_6$ cluster*

Fig. 1 depicts two predicted $NH_4^+(NH_3)_6$ isomers, 6I and 6II, which belong to the $C_{2v}$ and $C_s$ symmetry, respectively. 6I $(4+2)$ isomer contains two second shell $NH_3$ subunits attached to the first solvation shell by hydrogen bonding as $C_2$ axis symmetry. For 6II $(4+1+1)$ isomer, it contains one second shell $NH_3$ subunit and one third shell

$NH_3$ subunit as binding by hydrogen bonding. The B3LYP calculation indicated that isomer 6I is more stable than isomer 6II by 1.25 kcal/mol (Table 4). There exist two data sets for the b-NH bond length and the NH···N distance in both 6I and 6II and they are exactly opposite in phase (Table 1). In the case when NH···N ($NH_4^+$ ion) is cooperative with NHN (outer shell), the b-NH bond length is longer but the NH···N distance is shorter, compared to those in 4I.

The isomer 6II is calculated to see how intense the influence of ion. Due to the increased cooperative interactions of hydrogen bonding, the b-NH ($NH_4^+$ ion) bond is further lengthened and the NH···N ($NH_4^+$ ion) bond is shortened. It means that the additional hydrogen bond formation strengthens the interaction of NH···N ($NH_4^+$ ion). The results demonstrate the important role the cooperative effect plays in the hydrogen bonded systems.

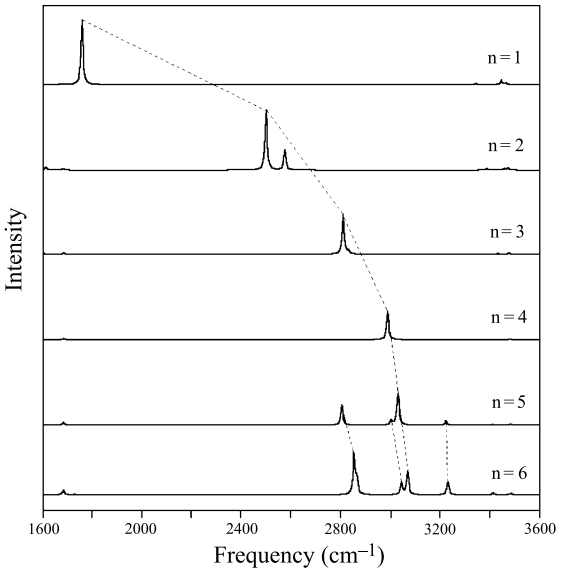


Fig. 4. Vibrational spectra of bonded NH stretching in $NH_4^+$ and $NH_3$, and the lowest energy isomers of $NH_4^+(NH_3)_n$ at $n = 1$–6 predicted by B3LYP/6-31G*.

### 3.2. Vibrational frequencies and IR spectra

The calculated NH stretching frequencies with B3LYP/6-31+G* and MP2/6-31+G* for the energy minimum structure of $NH_4^+(NH_3)_n$ $[n = 1$–$6]$ cluster are given in Table 5. The stretching frequencies of NH in the ammonium ion $NH_4^+(NH_3)_n$ clusters could be classified in terms of

(i) b-NH in $NH_4^+$ ion with hydrogen bonded to the nearest $NH_3$ molecule $[\nu_b(NH)_i]$,
(ii) f-NH in $NH_4^+$ ion $[\nu_f(NH)_i]$,
(iii) f-NH in $NH_3$ molecule $[\nu_b(NH)_n]$, and
(iv) b-NH in $NH_3$ molecule with hydrogen bonded to the nearest $NH_3$ molecule as second solvation shell $[\nu_f(NH)_n]$.

In this paper, we compare the stretching frequencies of the most stable isomer of $NH_4^+(NH_3)_n$ $[n = 1$–$6]$ cluster and ignore the other

Table 6
$\Delta H_n$ and $\Delta G_n$ (kcal/mol), of $NH_4^+ + nNH_3 \rightarrow NH_4^+(NH_3)_n$ at 298.15 K

| $NH_4^+(NH_3)_n$ | B3LYP/6-31+G* | | MP2/6-31+G* | | Expt. | |
|---|---|---|---|---|---|---|
| | $-\Delta H_n$ | $-\Delta G_n$ | $-\Delta H_n$ | $-\Delta G_n$ | $-\Delta H_n^o$ | $-\Delta G_n^o$ |
| 1I | 26.99 | 18.82 | 23.76 | 15.80 | 21.5[a], 27.0[b] | 15.5[a], 17.5[b] |
| 2I | 45.75 | 26.75 | 41.02 | 26.56 | 37.7[a], 44.0[b] | 24.9[a], 26.5[b] |
| 3I | 58.34 | 36.10 | 54.53 | 32.09 | 51. 2[a], 60.5[b] | 30.9[a], 32.9[b] |
| 3II | 54.78 | 29.39 | 48.83 | 27.13 | | |
| 4I | 69.06 | 36.31 | 65.61 | 36.09 | 62.9[a], 75.0[b] | 34.3[a], 36.7[b] |
| 4II | 65.69 | 36.50 | 61.20 | 32.74 | | |
| 4III | 62.12 | 29.54 | 56.05 | 27.21 | | |
| 5I | 76.52 | 36.88 | 71.78 | 36.13 | 69.9[a], 82.5[b] | 34.7[a], 37.2[b] |
| 6I | 83.41 | 33.73 | 78.19 | 29.90 | 76.4[a] | 34.7[a] |
| 6II | 81.72 | 32.73 | 76.48 | 30.56 | | |

[a] Ref. [37].
[b] Ref. [38].

isomers. The calculated frequencies are scaled by the factors 0.977 and 0.957 for B3LYP/6-31+G* and MP2/6-31+G*, level calculations, respectively, which are referred to the observed absorption of NH stretching in $NH_3$ [7]. Fig. 4 illustrates the calculated spectra of $NH_4^+(NH_3)_n$ at $n = 1$–4. The frequency red-shift of the b-NH stretching is great and the red-shift decreases as $n$ increases, an indication of the bond weakening of $NH\cdots N$ ($NH_4^+$ ion) as $n$ increases. The reduction of the red-shifts agrees well with the variation of the b-NH ($NH_4^+$ ion) bond length, the $NH\cdots N$ distances, and the interaction energies of $NH\cdots N$ hydrogen bonding with $n$. All these changes lead to the same conclusion that, as the number of $NH\cdots N$ ($NH_4^+$ ion) bonds increases, the anti-cooperative effect intensifies. While the changes in the $\nu_f(NH)_i$ frequencies are irregular, depending on isomers, the general pattern is in good accord with ion charge delocalization effects which force the $\nu_f(NH)_i$ to resonate at a higher frequency at a larger $n$. For $\nu_f(NH)_n$, the frequency changes are small and the trend of frequency shift is similar to that of the $\nu_n(NH)_i$ as $n$ increases. From the intuition of hydrogen bonding nature, the $NH_3$, as a proton acceptor, donor electrons to $NH_4^+$, which weakens the electron overlap of NH bond and causes the red-shift of f-NH stretching. As cluster size increases, the anti-cooperative of hydrogen bonding weakens the electron donating ability of $NH_3$, resulting in a smaller frequency red-shift.

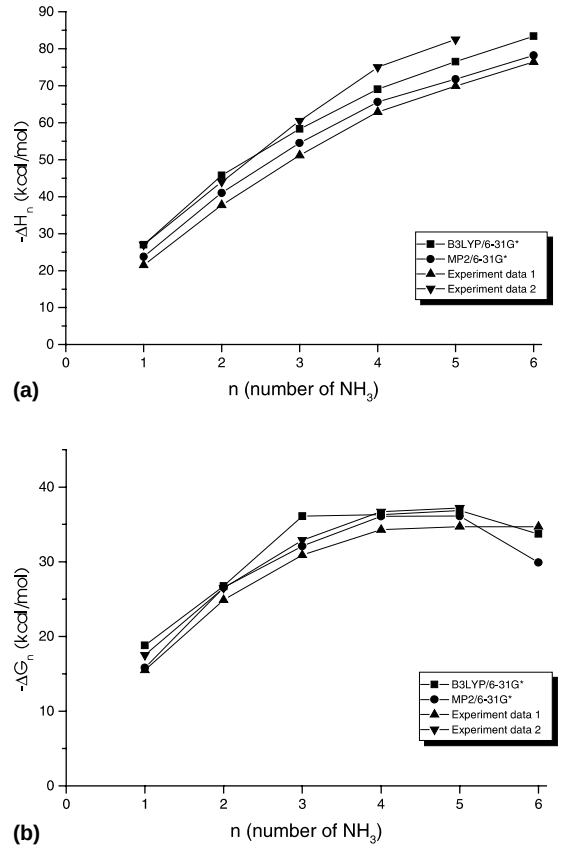


Fig. 5. Calculated hydration energies $-\Delta H_n$ and $-\Delta G_n$ of the lowest energy isomers of $NH_4^+(NH_3)_n$ at $n = 1$–6 using B3LYP/6-31G* and MP2/6-31G*.

### 3.3. Thermodynamic quantities

The calculated thermodynamic data, which included $-\Delta H_n$ and $-\Delta G_n$ values of the reactions $NH_4^+ + nNH_3 \rightarrow NH_4^+(NH_3)_n$, are tabulated in Table 6. These data contain the values of $-\Delta H_n$ and $-\Delta G_n$ generated through MP2 and B3LYP both using BSSE and ZPVE corrected energies. The predicted $-\Delta H_n$ and $-\Delta G_n$ values with respect to the experimental results are given in Fig. 5. Noticeably, the predicted values of $-\Delta H_n$ and $-\Delta G_n$ for the dominant species by B3LYP/6-31+G* are always larger than those by MP2/6-31+G*. The prediction of interaction energies from ab initio calculations falls in the range of the observations. It is noted, however, that the difference in prediction between these two methods gradually reduces as $n$ increases. Since no more ionic-hydrogen bond can be formed, there exists discontinuity in the heat of hydration ($\Delta H_n$) for the clustering, $NH_4^+ + nNH_3 \rightarrow NH_4^+(NH_3)_n$, at $n = 4$.

## 4. Conclusions

Both B3LYP/6-31+G* and MP2/6-31+G* methods have been applied to investigate the geometries, energies and vibrational spectra of $NH_4^+(NH_3)_n$ structural isomers at $n \leqslant 6$ throughout this work. Results indicate that ion–dipole interactions dominate the solvation process of $NH_4^+(NH_3)_n$ before the first solvation shell is

completely filled, whereas the second shell hydration is primarily determined by the hydrogen bonding interactions between $NH_3$ molecules. The interaction energies of the important species decrease monotonously and the discontinuity exists as the second shell solvation occurs.

In the solvation processes, there are many properties, such as geometries, interaction energies and vibrational frequencies, that are influenced by the nonadditivity of hydrogen bonding interactions. The cooperative interactions, where bridge molecule is both proton donor and acceptor, will enhance the interactions of hydrogen bondings which cause the b-NH stretching more red-shift, the lengthening of the b-NH and shortening the distance of hydrogen bonds. Whereas, anti-cooperative interactions, where $NH_4^+$ plays a role as a multiple proton donor, will weaken the interactions of hydrogen bondings which cause the reverse influences on the b-NH stretchings, the bond lengths of the b-NH and the distances of hydrogen bonds.

The higher level calculations show nearly free internal rotation of $NH_3$ molecules about their local $C_3$ axes in the first solvation shell and it is in good agreement with the prediction by VPS [7]. Our calculations also reveal that $N_2H_7^+$ ion does not exist in the $NH_4^+(NH_3)_n$ clusters.

## Acknowledgements

The authors thank the National Science Council of Taiwan, R.O.C. and the Academia Sinica for Financial support.

## References

[1] R.S. Narcisi, A.D. Bailey, J. Geophys. Res. 70 (1965) 3687.
[2] E.E. Ferguson, F. Arnold, Acc. Chem. Res. 14 (1981) 327.
[3] M.D. Perkins, F.L. Eisele, J. Geophys. Res. 80 (1984) 9649.
[4] J.C. Jiang, H.-C. Chang, Y.T. Lee, S.H. Lin, J. Phys. Chem. 103 (1999) 3123.
[5] Y.-S. Wang, J.C. Jiang, C.-L. Cheng, S.H. Lin, Y.T. Lee, H.-C. Chang, J. Chem. Phys. 107 (1997) 9695.
[6] J.M. Price, M.W. Crofton, Y.T. Lee, J. Chem. Phys. 91 (1989) 2749.
[7] J.M. Price, M.W. Crofton, Y.T. Lee, J. Phys. Chem. 95 (1991) 2182.
[8] H.-C. Chang, J.C. Jiang, S.H. Lin, Y.T. Lee, H.-C. Chang, J. Phys. Chem. 103 (1999) 2941.
[9] H.-C. Chang, J.C. Jiang, S.H. Lin, Y.T. Lee, H.-C. Chang, J. Am. Chem. Soc. 121 (1999) 4443.
[10] H.-C. Chang, J.C. Jiang, S.H. Lin, Y.T. Lee, H.-C. Chang, Isr. J. Chem. 39 (1999) 231.
[11] C.-C. Wu, J.C. Jiang, D.W. Boo, S.H. Lin, Y.T. Lee, H.-C. Chang, J. Chem. Phys. 112 (2000) 176.
[12] C. Chaudhuri, J.C. Jiang, X. Wang, Y.T. Lee, H.-C. Chang, J. Chem. Phys. 112 (2000) 7279.
[13] J.C. Jiang, H.-C. Chang, Y.-S. Wang, S.H. Lin, Y.T. Lee, H.-C. Chang, G.N. Schatteburg, J. Am. Chem. Soc. 122 (2000) 1398.
[14] Y.-S. Wang, H.-C. Chang, J.C. Jiang, S.H. Lin, Y.T. Lee, H.-C. Chang, J. Am. Chem. Soc. 120 (1998) 9695.
[15] L.I. Yeh, M. Okumura, J.D. Myers, J.M. Price, Y.T. Lee, J. Chem. Phys. 91 (1989) 7319.
[16] J.-H. Choi, K.T. Kuwata, B.-M. Hass, Y. Cao, M.S. Johnson, M.J. Okumura, Chem. Phys. 100 (1994) 7153.
[17] K. Hirao, T. Fujikawa, H. Konishi, S. Yamabe, Chem. Phys. Lett. 104 (1984) 184.
[18] M.J. Meot-Ner, Am. Chem. Soc. 106 (1984) 1265.
[19] (a) P.A. Kebarle, Rev. Phys. Chem. 28 (1977) 455;
(b) J.D. Payzant, A.J. Cunningham, P. Kebarle, Can. J. Chem. 51 (1973) 3242.
[20] D.A. Armstrong, A. Rauk, D. Yu, Can. J. Chem. 71 (1993) 1368.
[21] E. Kassab, E.M. Evleth, Z.D. Hamou-Tahra, J. Am. Chem. Soc. 112 (1990) 103.
[22] (a) M. Welti, T.-K. Ha, E.J. Pretsch, Chem. Phys. 83 (1985) 2959;
(b) L. Jaroszewski, B. Lesyng, J.A. McCammon, J. Mol. Struct. (Theochem) 283 (1993) 57;
(c) L. Jaroszewski, B. Lesyng, J.J. Tanner, J.A. McCammon, Chem. Phys. Lett. 175 (1990) 282;
(d) A. Pullman, P. Claverie, M.-C. Cluzan, Chem. Phys. Lett. 117 (1985) 419;
(e) A. Pullman, A.M. Armbruster, Int. J. Quantum Chem. 11 (1977) 701.
[23] J.C. Contador, M.A. Aguilar, F.J. Olivares del Valle, Chem. Phys. 214 (1997) 113.
[24] H.-H. Bueker, E. Uggered, J. Phys. Chem. 99 (1995) 5945.
[25] M.D. Newton, S. Ehrenson, J. Am. Chem. Soc. 93 (1971) 4971.
[26] E.D. Glendening, D. Feller, J. Phys. Chem. 99 (1995) 3060.
[27] E. Magnusson, J. Phys. Chem. 98 (1994) 12558.
[28] J. Kim, S. Lee, S.J. Cho, B.J. Mhin, K.S. Kim, J. Chem. Phys. 102 (1995) 839.
[29] C.W. Bauschlicher, S.R. Langhoff, H. Partridge, J.E. Rice, A. Komornicki, J. Chem. Phys. 95 (1991) 5142.
[30] D. Feller, E.D. Glendening, R.A. Kendall, K.A. Peterson, J. Chem. Phys. 100 (1994) 4981.
[31] Y. Xie, R.B. Remington, H.F. Schaefer III, J. Chem. Phys. 101 (1994) 4878.
[32] A. Bagno, V. Conte, F.D. Furia, S. Moro, J. Phys. Chem. A 101 (1997) 4637.

[33] M.J. Frisch et al., Gaussian 94, Revision D.3, Gaussian Inc., Pittsburgh, PA, 1995.
[34] S.F. Boys, F. Bernardi, Mol. Phys. 19 (1970) 553.
[35] W.S. Benedict, E.K. Plyler, E.D. Tidwell, J. Chem. Phys. 32 (1960) 32.
[36] I.N. Tang Jr., A.W. Castleman, J. Chem. Phys. 62 (1972) 4576.
[37] M.R. Arshadi, J.H. Futrell, J. Phys. Chem. 78 (1974) 1482.
[38] S.K. Searles, P. Kebarle, J. Phys. Chem. 72 (1986) 742.